Study on the Generalized Formulations with the Aim to Reproduce the Viscoelastic Dynamic Behavior of Polymers

Andrea Genovese *[ID]**, Francesco Carputo, Antonio Maiorano, Francesco Timpone, Flavio Farroni**[ID] **and Aleksandr Sakhnevych**[ID]

Department of Industrial Engineering, University of Naples Federico II, Via Claudio, 21-80125 Naples, Italy; francesco.carputo@unina.it (F.C.); antonio.maiorano@unina.it (A.M.); francesco.timpone@unina.it (F.T.); flavio.farroni@unina.it (F.F.); ale.sak@unina.it (A.S.)
* Correspondence: andrea.genovese2@unina.it

Abstract: Appropriate modelling of the real behavior of viscoelastic materials is of fundamental importance for correct studies and analyses of structures and components where such materials are employed. In this paper, the potential to employ a generalized Maxwell model and the relative fraction derivative model is studied with the aim to reproduce the experimental behavior of viscoelastic materials. For both models, the advantage of using the pole-zero formulation is demonstrated and a specifically constrained identification procedure to obtain the optimum parameters set is illustrated. Particular emphasis is given on the ability of the models to adequately fit the experimental data with a minimum number of parameters, addressing the possible computational issues. The question arises about the minimum number of experimental data necessary to estimate the material behavior in a wide frequency range, demonstrating that accurate results can be obtained by knowing only the data of the upper and low frequency plateaus plus the ones at the loss tangent peak.

---

1. Introduction

Viscoelasticity regards the study of materials exhibiting a time dependence behavior. The knowledge of the viscoelastic properties of these materials is at the basis of a correct analysis of structures, where the viscoelastic materials are employed, especially when dealing with dynamic phenomena and vibrations. Materials with viscoelastic behavior are widely employed in many different applications starting from biological tissues, such as the disks in the human spine [1] and skin tissue [2,3], up to civil and industrial systems such as elastomers. As regards the latter field of study, tall buildings are damped with viscoelastic materials to avoid instabilities and to face vibration problems caused by wind or earthquakes [4,5]. Viscoelastic dampers have long been used in the control of vibration and noise in aerospace structures and industrial machines. In many mechanical systems, such materials are widespread and used for damping and insulation scope [6], i.e., they are used in automobile bumpers, machine insulation, to protect computer drives from mechanical shocks and are also used in shoe insoles to reduce impact transmitted to the person and to increase comfort. Moreover, materials that behave elastically at room temperature often show significant viscoelastic properties when heated. In addition, tires are made of different polymers and elastomers with peculiar viscoelastic properties responsible for many tire/road interaction phenomena that affect vehicle dynamics in term of safety and performance. Friction performance [7,8], rolling resistance and wear are some examples of events in which the viscoelasticity of the tread plays a fundamental role.

The characterization of these materials involves two main phases: experimental tests and analytical modelling. A good understanding of the dynamical behavior of structures where viscoelastic materials are used is strictly dependent on their rheological properties and on some of their geometric parameters. These characteristics in turn depend on the temperature and on the induced excitation frequency quantities. Material models and simulation tools become fundamental to understand and to reduce uncertainties during the earliest phases of the material development, optimizing the design of composite and multi-layered material components and the manufacturing process. Furthermore, the possibility to employ realistic models of materials allows to make reliable predictions of the behavior of existing components as well as for those in the process of development.

To define a constitutive law for linear viscoelasticity, at least three different common approaches can be adopted: integral models, linear differential models and fractional derivative models. The basic foundation of linear viscoelasticity theory is the Boltzmann's superposition principle according to which every loading step makes an independent and additive contribution to the final state [9]. This idea can be used to formulate an integral representation of linear viscoelasticity. Nevertheless, a more convenient and widespread way to describe the linear viscoelasticity is the differential approach, where a combination of mechanical elements, ideal springs and dashpot, are used to describe the rheological properties. On one hand, spring is a perfect elastic element, following Hooke's law and behaving like an elastic solid; on the other hand, dashpot is a perfect viscous element, following Newton's Law. The methodology links stress and strain through linear differential equation. The simplest and most famous models currently employed are the Maxwell model, Kelvin–Voigt model and Zener model. However, Maxwell model fails in reproduction of the creep phenomenon and Kelvin–Voigt model fails in the description of the relaxation behavior [10]. Furthermore, in terms of frequency domain, both models are efficient only within a small frequency range, but they become insufficient within low and high frequency ranges, representing an important limit in case the specific application could require different boundary conditions in terms of excitation frequency to be applied on the same material model.

When the deformations of a viscoelastic material are neither small nor very slow, its behavior is no longer linear, and there is no universal rheological constitutive equation that can predict the response of the material to such a deformation. Hence, for modelling their behavior in these cases, finite strain-based viscoelastic models are required. Some notable studies can be found in literature regarding finite viscoelastic modelling of polymers. The finite strain thermo-viscoelastic constitutive model, proposed by Liao et al. [11] employs a non-linear evolution law based on the classical concept of the multiplicative decomposition of the deformation gradient using specific hyper-elastic parameters identified at reference temperature values. Following the Bergstrom–Boyce model for nonlinear finite rubber viscoelasticity [12], Hossain et al. proposed a modified version of the micro-mechanically motivated Bergstrom–Boyce viscoelastic model used along with a finite linear evolution law [13], while a model for rate-dependent phenomena in elastomers founded on finite strain theories in consistence with the natural laws of thermodynamics is proposed in [14].

In order to get around the specific characterization procedures, generalized models are often employed allowing to describe the viscoelastic behavior of the materials in a wide range of frequencies and time scales. The above models, consisting of a combination of a number of elementary springs and dashpots, generally known as the Generalized Maxwell model (GM) and generalized Kelvin–Voigt model (GKV), offer a good description of the real viscoelastic material but they consist of a considerable amount of appropriately connected spring and dashpot elements. This means that a set of differential equations must be solved to evaluate the dynamic behavior of the components under investigation [15], which could considerably complicate the mathematical formulation describing the dynamic state of the system and might significantly increase the computational load due to a larger set of motion equations to be solved. To overcome these issues, fractional models are becoming more and more popular because of their ability to describe the behavior of viscoelastic materials using a limited number of parameters with an acceptable accuracy over a vast range of excitation frequencies. Several authors have put

the focus on the modelling approach based on fractional calculus allowing the characterization of rheological behavior of linear viscoelastic systems [16–20], pointing out several significant problems connected with the robust identification of model parameters.

The parameters' identification procedure can be classified according to the data domain employed (time-based or frequency-based) and according to the methods employed. Time-domain-based identification procedures can exploit creep and relaxation experimental tests [21], hysteresis loops of steady-state harmonic experimental tests [22] and impact tests [23]. Frequency-domain-based procedures can exploit magnitude and phase of the frequency response function [24] or the definition of storage modulus and loss factor [25,26]. Recently, Shabani et al. [27] have proposed a new frequency-domain-based identification procedure defining an ad-hoc testing setup. As concerns the classification by the identification method, an accurate literature review points out that the authors generally adopt a multitude of different procedures, i.e., Arikolu [26] and Zhou et al. [28] have proposed a genetic algorithm method, while procedure based on a curve fitting has been used by de Espindola et al. [25] and Sasso et al. [19]. A classical approach based on minimization of a proposed cost function has been explored by Yuan and Agrawal [29] while, more recently, ant colony optimization method [30] and spectral parameter estimation approach have been also investigated [31].

However, it must be highlighted that these references generally assess the goodness of the model behavior towards ideal and virtual materials acknowledging the potential of the mathematical formulation under study to describe a vast frequency range or the validation is obtained towards very limited experimental data of the material viscoelastic response. For this reason, to assess a generalized model and its robust parameter identification procedure to reproduce the experimental data of dynamic tests (in a wide range of frequency values), with a unique set of parameters, the aim of this work is to discover the optimum model formulation that can describe the real viscoelastic behavior with a minimum number of parameters. To this purpose, three completely different polymers have been considered to compare the response of two chosen models: the Generalized Maxwell model (GM) and the relative fractional derivative model (FDGM). For the both models, the parameters' optimum sets have been identified adopting a pole-zero formulation introduced by Renaud et al. in [32], limited to the case of the GM model. Furthermore, once the best model formulation has been discovered, a further study on the minimum amount of experimental data and their distribution within the frequency domain, necessary to correctly reproduce the materials' viscoelastic behavior in a wide frequency range with an acceptable accuracy, has been carried out.

The paper is organized as follows: in Section 2, the experimental data, employed as an experimental reference dataset for the study, are presented; in Section 3, the rheological models adopted are presented starting from their definition in the time domain and their re-definition in the frequency domain to obtain the relative pole-zero formulation; in Section 4, the parameters' identification procedure developed to achieve the fitting of the experimental data is presented; in Section 5, the model comparison in terms of the dynamic response and the ability to reproduce the viscoelastic behavior of the compounds under analysis are illustrated; in Section 6, a specific study to understand how the minimum number of experimental points should be acquired and distributed to identify the model parameter set in a robust way is reported.

2. Materials Experimental Data

The viscoelastic material is a deformable material with a behavior which lays between a viscous liquid and an elastic solid. Their behavior deviates from Hooke's elastic law, exhibiting both elastic and viscous characteristics at the same time. In this kind of materials, the stress–strain relationship is a function of time and the viscoelastic characteristics exhibit time-dependent behavior and load application speed at an established temperature value.

To better understand the mechanical behavior in viscoelastic materials, two main types of experiments are usually carried out: transient and dynamic. While static characterization regards the quasi-static application of load or deformation, transient and dynamic testing procedures concern the

analysis of material response to a time applied deformation or load function (elongation or shear). Two important categories regarding the transient material testing are commonly performed: the creep experiment and stress-relaxation experiment.

In the creep experiment, the material is subjected to uniform load to analyze the strain time changes while during the stress-relaxation experiment, the material is subjected to a fixed deformation and the load required to maintain the deformation at a constant value is measured with time. The above transient tests allow to characterize the viscoelastic material reaction for each applied stress–strain load step.

Another important testing procedure class able to describe the viscoelastic behavior consists of the dynamic experiments. These tests are commonly employed to analyze the material reaction to cyclic stress (1) or strain applied:

$$\sigma(t) = \sigma_0 \sin \omega t \tag{1}$$

where ω represents the angular frequency of an applied sinusoidal stress and depends on the time. In quasi-elastic materials, the strain generated by the stress also exhibits a sinusoidal trend with the same phase of the applied load. On the opposite side, in viscoelastic materials, the strain reaction shows a time delay towards the applied stress, characterized by a phase angle δ. Therefore, the strain response is given by (2):

$$\varepsilon(t) = \varepsilon_0 \sin(\omega t - \delta) \tag{2}$$

Because of the phase displacement, the material dynamic stiffness can be considered as a complex variable E^* according to Euler's formulation (3):

$$\frac{\sigma(\omega)}{\varepsilon(\omega)} = E^* = E' + E'' \tag{3}$$

where E' is the storage modulus [Pa] and E'' is the loss modulus [Pa].

These quantities are deeply linked to the way the material dissipates a part of energy provided by means of a load/stress time function. They are related to the phase angle δ, according to the following Equation (4):

$$\frac{E''(\omega)}{E'(\omega)} = \tan \delta \tag{4}$$

The phase angle tangent δ is also called loss tangent. It is important to remark that all the quantities, referring to the viscoelastic behavior, are function of the frequency at which the sinusoidal load/deformation is applied and of the material temperature.

Hereafter, the output of dynamic mechanical analysis (DMA) [33] for the moduli characterization of three different polymers called A, B and C is reported. Such testing procedure prescribes an oscillatory deformation of the material sample with a constant strain or stress amplitude in order to measure the viscoelastic modulus. The oscillatory load is applied at different frequencies and then repeated at different temperatures. The master curves at a chosen reference temperature and over a wide range of frequencies is obtained exploiting the time–temperature superposition principle [34], which allows to shift the results measured at different temperatures. For each polymer, the real part of the Young's modulus and the tan δ are reported in Figure 1a,b, respectively, at the reference temperature of 120 °C.

The characteristics of the three polymers, which are summarized in the Table 1, show that these materials describe a wide range of application of polymers, having different characteristics from each other. In the table, T_g is glassy transition temperature, E_∞ is the glassy region dynamic modulus (the dynamic modulus at high frequency) and E_0 is rubbery region modulus (the dynamic modulus at low frequency).
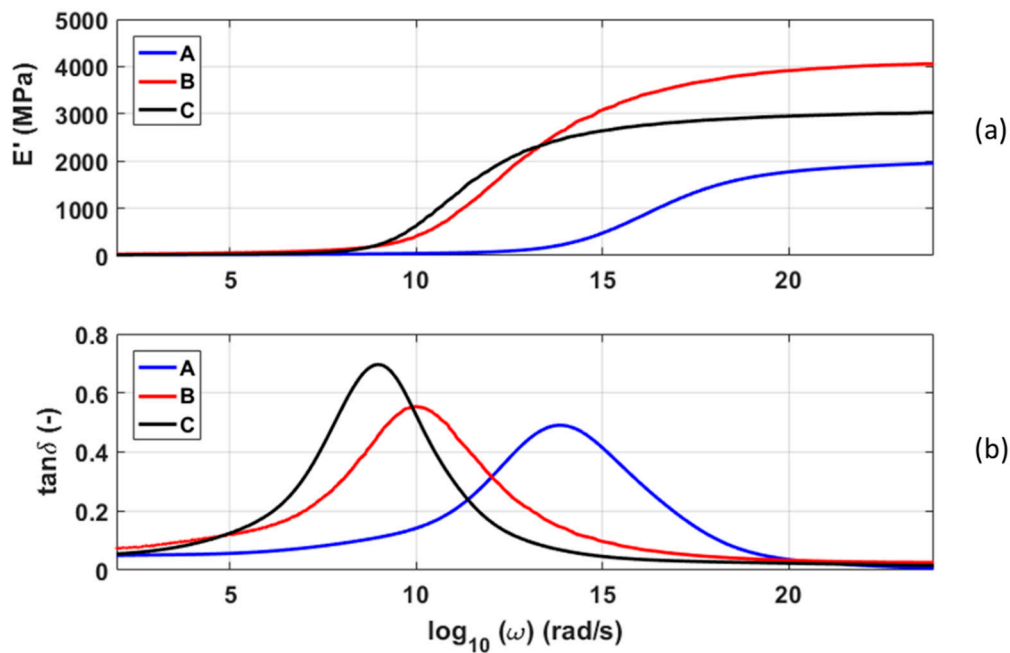
Figure 1. Storage modulus (a) and loss tangent (b) of rubber compounds A, B and C at a reference temperature T_{ref} =120°.

Table 1. Principal characteristics of the three studied polymers

POLYMER	T_g (°C)	E_∞ (MPa)	E_0 (MPa)
A	−27	1588	7.9
B	−16	4057	22.3
C	−10	3031	12.03

3. Rheological Models

For the purpose of understanding and describing of the material viscoelastic behavior, different mathematical models have been developed and are available in the literature. Since the experimental characterization of the viscoelasticity of the compounds is particularly important to properly feed the procedures of so many different application areas, the question arises about which could be the analytical model that is able to reproduce the viscoelastic behavior in an optimal and robust way employing the minimum number of parameters. In other words, the aim is to investigate the simplest constitutive model able to reproduce the experimental viscoelastic behavior in the widest range of operating frequencies.

The simple Maxwell or Kelvin models fail in representing the actual response of viscoelastic materials at low and high frequencies, respectively, while the generalized models are able to provide more reliable results. As this paper is focused on viscoelastic solids, the GM model and FDGM model are considered and refer to a spring in parallel with (respectively) Maxwell cells and fractional Maxwell cells as defined by Koeller [35]. Maxwell cells are composed of a spring and a dashpot arranged in series, while the fractional Maxwell element is obtained by replacing the dashpot elements with the so-called spring-pot elements. Figure 2 depicts the rheological model considered.

In the following chapters, the GM and FDGM models are mathematically described. Starting from the models' definition in the time domain, the frequency domain expressions are derived by means of the Fourier transform to obtain the pole-zero formulation of both the models under analysis.
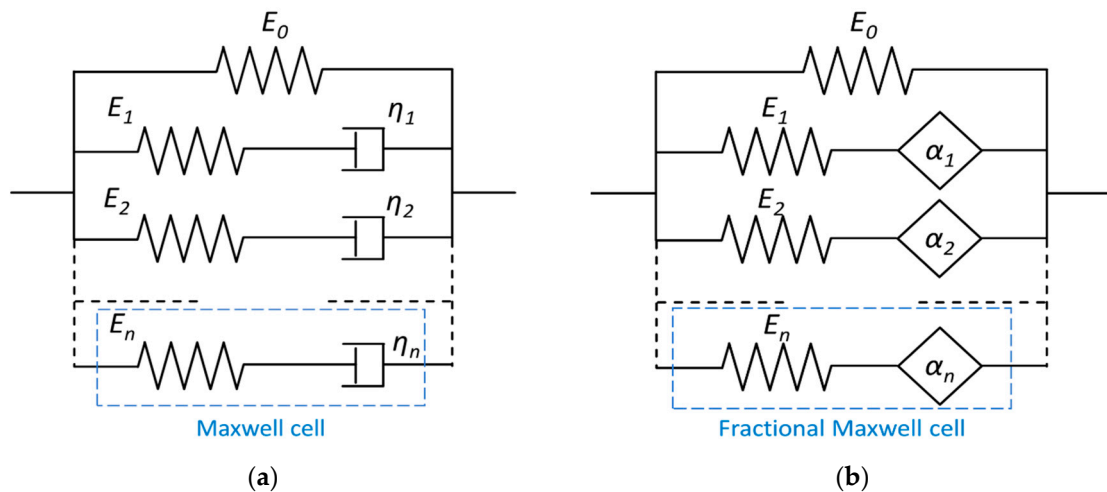
Figure 2. Models: (a) Generalized Maxwell, (b) Fractal derivative.

3.1. Generalized Maxwell Model

The differential equation for of the GM model formulation can be expressed in the general form as

$$\sum_{n=0}^{N} a_n \frac{d^n \sigma(t)}{dt^n} = \sum_{m=0}^{M} b_m \frac{d^m \varepsilon(t)}{dt^m} \tag{5}$$

where the parameters $b_0 = 0$ and $N = M$ are assumed for the considered case of Maxwell model. The complex modulus can be derived transforming Equation (5) into the frequency domain. Calculating the Fourier transform of (5), the following expression for the complex moduli is derived:

$$E^*(i\omega) = E_0 + \sum_{k=1}^{N} \frac{i\omega E_k \eta_k}{E_k + i\omega \eta_k} \tag{6}$$

where the parameters E_k and η_k represent the springs stiffness and dashpots viscosity, respectively, as represented in Figure 2a, and ω is the angular frequency.

Renaud et al. [32] have demonstrated that the GM model, mathematically described in (6) in a frequency domain, can be equivalently expressed in the pole-zero formulations as in (7):

$$E^*(i\omega) = E_0 \prod_{k=1}^{N} \frac{1 + \left(\frac{i\omega}{\omega_{z,k}} \right)}{1 + \left(\frac{i\omega}{\omega_{p,k}} \right)} \tag{7}$$

where ω_z and ω_p are the zero and pole, respectively.

3.2. Fractal Derivative Generalized Maxwell Model

A generic constitutive equation for viscoelastic materials based on fractional derivative orders is expressed in the following form:

$$\sum_{n=0}^{N} a_n \frac{d^{\alpha_n} \sigma(t)}{dt^{\alpha_n}} = \sum_{m=0}^{M} b_m \frac{d^{\beta_m} \varepsilon(t)}{dt^{\beta_m}} \tag{8}$$

where α_n and β_m are the fractional derivative orders included between 0 and 1, $N=M$ and $b_0=0$ for the considered case of Maxwell model. Turning to frequency domain, and assuming that $\alpha = \beta$, Equation (8) becomes:

$$E^*(i\omega) = E_0 + \sum_{k=1}^{N} \frac{(i\omega)^{\alpha_k} E_k \eta_k}{E_k + (i\omega)^{\alpha_k} \eta_k} \tag{9}$$

In analogy with the GM model, (9) can be equivalently expressed in the pole-zero formulations as in (10):

$$E^*(i\omega) = E_0 \prod_{k=1}^{N} \frac{1 + \left(\frac{i\omega}{\omega_{z,k}}\right)^{\alpha_k}}{1 + \left(\frac{i\omega}{\omega_{p,k}}\right)^{\alpha_k}} \tag{10}$$

4. Identification Procedure

The term *pole-zero identification* refers to the achievement of the poles and zeros of a linear, or linearized, system described by its frequency response. This is usually done using optimization techniques able to fit a given frequency response of the linear system towards a transfer function defined as the ratio of two polynomials [36,37]. This kind of linear system identification in the frequency domain has several applications in a wide variety of engineering fields and it can be constrained or unconstrained.

In this work, the pole-zero identification is performed adopting a constrained procedure taking advantage from the "fminmax" Matlab function that seeks the minimum of a nonlinear error function W of n real variables, the Zeros and the Poles. For the present identification problem, this function will be defined as the weighted sum of the normalized root mean square error (NRMSE) calculated for the storage modulus and the loss tangent as in (11):

$$W = (1 - r) \cdot Err_E + r \cdot Err_{tan\delta} \tag{11}$$

where r is the weight factor and $Err_{tan\delta}$ and Err_E are defined by (12)

$$Err_{tan\delta} = \frac{\sqrt{\frac{\sum_{i=1}^{N}(tan\delta - tan\delta_{model})^2}{N}}}{mean(tan\delta)} \quad Err_E = \frac{\sqrt{\frac{\sum_{i=1}^{N}(E - E_{model})^2}{N}}}{mean(E)} \tag{12}$$

Notice that this way of defining the error function allows to fit both modulus and phase at the same time. As concerns the weighting coefficient r, generally, it can be set equal to the more convenient value in order to have the more robust results. In the present paper, the weighting coefficient r has been assumed equal to 0.5 for all identifications in order to compare the results of different procedures.

The function W must be constrained imposing that the poles p and zeros z are alternate, according to the third property demonstrated by Bland [38] for linear dissipative systems (13):

$$z_1 < p_1 < z_2 < p_2 < z_3 < p_3 \ldots < z_i < p_i \tag{13}$$

As concerns the initial condition of the identification procedure, the initialization of the pole-zero parameters has been carried out by means the method proposed by Renaud et al. [32]. Dividing the frequency domain into N equal frequency subdomains each Pole Zero couple is given by (14):

$$\begin{cases} \omega_{z,i} = (1-r) \cdot \omega_{z,i}^{Modulus} + r \cdot \omega_{z,i}^{Phase} \\ \omega_{p,i} = (1-r) \cdot \omega_{p,i}^{Modulus} + r \cdot \omega_{p,i}^{Phase} \end{cases} \tag{14}$$

where, posing $\chi = \log_{10}(\omega)$, $\omega_{z,i}$ and $\omega_{p,i}$ for modulus and phase are calculated as in (15):

$$\begin{cases} \chi_{z,i}^{Modulus} = \chi_{c,i} - \frac{\alpha_i}{2} \\ \chi_{P,i}^{Modulus} = \chi_{c,i} + \frac{\alpha_i}{2} \end{cases} ; \quad \begin{cases} \chi_{z,i}^{Phase} = \chi_{c,i} - \frac{\alpha_i}{2} \\ \chi_{P,i}^{Phase} = \chi_{c,i} + \frac{\alpha_i}{2} \end{cases} \tag{15}$$

where $\chi_{c,i}$ is the medium frequency of a couple and α_i is evaluated considering the stiffing of the modulus $|E^*(\omega)|$ and the area under the phase curve the $\delta(\omega)$ defined respectively as in (16) and (17):

$$S = \alpha_i = \int_{\chi a,i}^{\chi b,i} \frac{d}{d\chi} \left(\log_{10} |E*(\chi)| \right) d\chi \tag{16}$$

$$A = \alpha_i \cdot \frac{\pi}{2} = \int_{\chi a,i}^{\chi b,i} \delta(\chi) d\chi \tag{17}$$

From the computational point of view, the convenience of the pole zero formulation in the identification of parameters of transfer functions lies in how the boundary conditions and the initial conditions of the optimization problem can be defined. As an example, using the formulation (6) of the GM model, the parameters to be identified are stiffness and damping coefficients. Hence, defining both the initial conditions and the boundary conditions is a hard task because they can vary between zero and very large numbers and as a function of the elements of the model itself. Using a pole-zero formulation, it is easier to define the initial conditions, i.e., by means of Equation (14). Moreover, the range of parameters to be identified (poles and zeros) is defined and limited by the frequency range of the experimental curves and this condition greatly facilitates the optimization algorithm efficiency.

5. Models Analysis

The identification procedure described in the previous paragraph has been employed to evaluate the capability of the GM and FDGM models to describe three completely different viscoelastic materials. Moreover, for each model, we need to understand the minimum number of parameters that can describe the dynamic characteristics of the considered viscoelastic materials. Therefore, to this purpose, the identification procedure has been performed for each model considering an increasing number of elements until the fitting of experimental data was not satisfactory.

To quantitatively compare the models presented in this paper, the NRMSE is evaluated for the storage modulus and the loss tangent quantities as defined in Equation (12). The purpose of these indicators is to quantify the goodness of the models' behavior towards the experimental data reproduction.

Figure 3 compares experimental data with the results obtained for the three compounds with the GM models composed by 15, 25 and 35 elements plus a spring in parallel (E_0 in Figure 2), while in Table 2, the relative calculated NRMSEs are reported.

Table 2. NRMSEs for Generalized Maxwell models composed by 15, 25 and 35 elements.

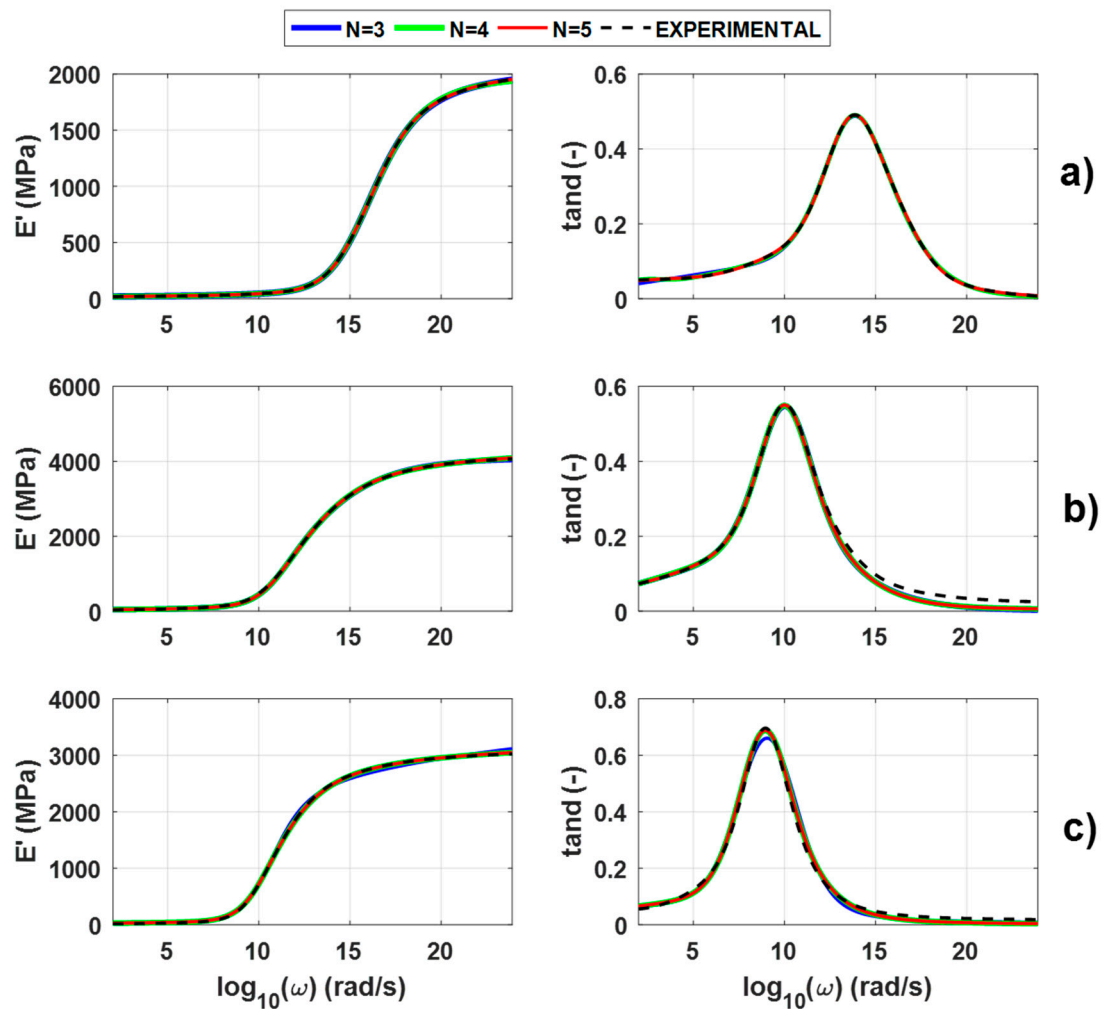| GM model	Compound A		Compound B		Compound C	
	NRMSE E′ (MPa)	NRMSE tanδ (-)	NRMSE E′ (MPa)	NRMSE tanδ (-)	NRMSE E′ (MPa)	NRMSE tanδ (-)
15 elements	0.0183	0.0876	0.0416	0.1146	0.0279	0.2358
25 elements	0.0038	0.0148	0.0306	0.0822	0.0087	0.2355
35 elements	0.0021	0.0053	0.0305	0.0789	0.0069	0.2352
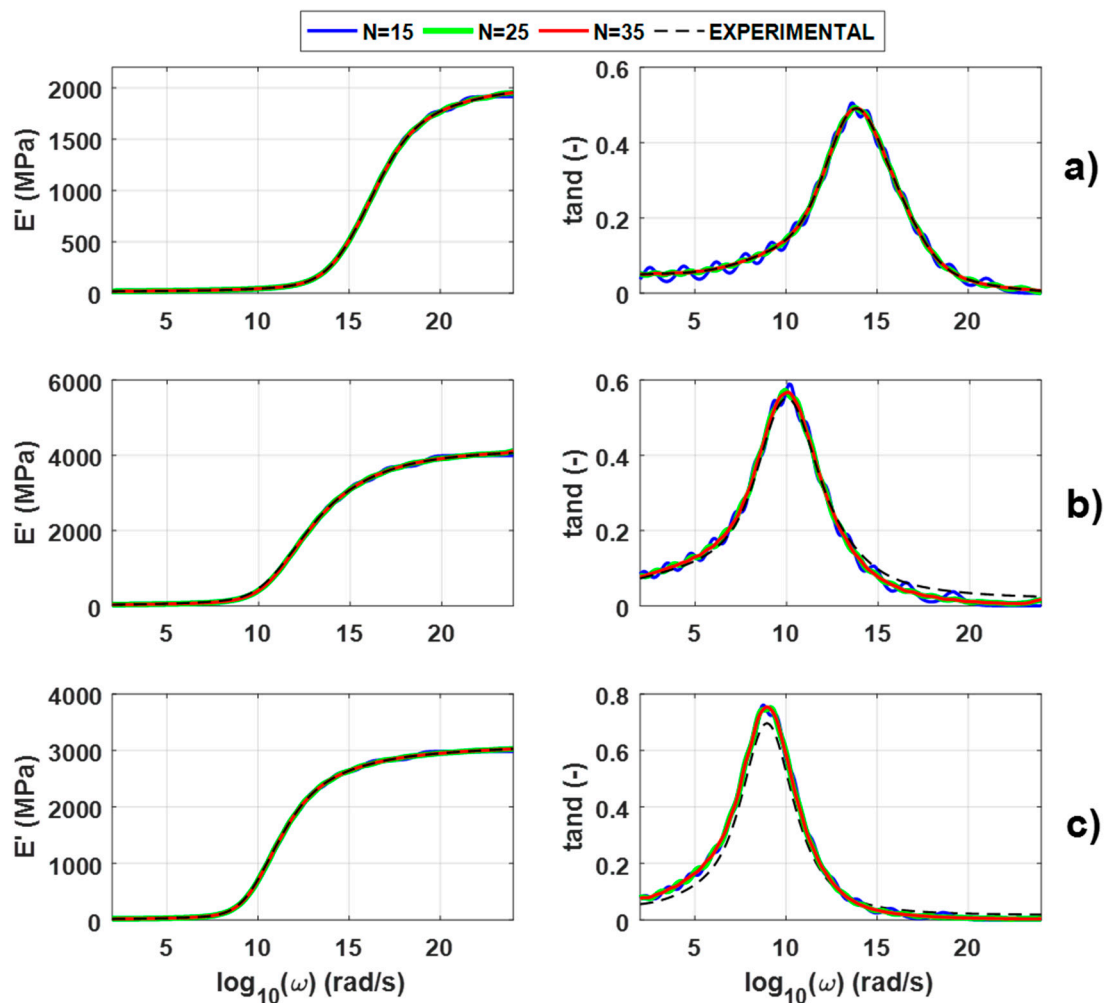
Figure 3. Storage modulus and loss tangent for compounds A (a), B (b) and C (c): experimental data (dashed line) vs. GM model with 15 (blue line), 25 (green line) and 35 (red line) elements.

The identified parameters of these models are detailed in Tables A1–A3 in Appendix A. Analyzing the models' results, it is evident that the GM model composed of 15 elements appears totally insufficient to describe the compounds' frequency response because it shows unphysical local oscillations although it seems to follow the real global trend. As highlighted by the NRMSE in Table 2, by increasing the number of Maxwell elements, the fitting of experimental data is improved as well. However, it should be noted that to have significant improvements in model results, several elements must be added with a consequent increase in the parameters to be identified.

The FDGM model results are reported in Figure 4. For each compound, the experimental data are compared with models composed by a spring (E_0 in Figure 2) in parallel with 3, 4 and 5 spring-pot elements. The corresponding NRMSEs are reported in Table 3, while the parameters of these models are detailed in Tables A4–A6 in Appendix A. It should be noted that the FDGM model is able to give an acceptable representation of the curves' shapes with a three-element model which is also consistent with the NRMSE values. Also in this case, increasing the number of model elements, the fitting of experimental data improve.

Figure 4. Storage modulus and loss tangent for compound A (a), B (b) and C (c): experimental data (dashed line) vs. FDGM model with three (blue line), four (green line) and five (red line) elements.

Table 3. NRMSEs for Fractal Derivative Generalized Maxwell models composed of 3, 4 and 5 elements.

	Compound A		Compound B		Compound C	
FDGM model	NRMSE E' (MPa)	NRMSE tanδ (-)	NRMSE E' (MPa)	NRMSE tanδ (-)	NRMSE E' (MPa)	NRMSE tanδ (-)
3 elements	0.0028	0.0273	0.0187	0.059	0.0513	0.1054
4 elements	0.0059	0.012	0.0176	0.0574	0.0251	0.0822
5 elements	0.002	0.0038	0.0178	0.0568	0.0251	0.0821

A relative comparison between the three compounds shows that, regardless of the model used, compound A returns the best fitting results than the others for the same number of elements used. By mere comparison of normalized errors, we observed (in general) a good performance of both models adopted in describing the real compounds' behavior, but GM model needs a greater number of elements than the FDGM. While FDGM was able to provide good matching with the simple configuration with only ten unknowns, for the GM, it was necessary to build up a more complicated model by adding several elements. Indeed, in terms of parameters to identify, each element of GM requires two parameters (1 pole-zero couple), while for FDGM, each one needs three parameters (1 pole-zero couple and the fractal derivative order α). This means that a 15-elements GM implies 31 parameters to be identified; the 15 pole-zero couples and the E_0. Similarly, a three-elements FDGM needs ten parameters

to be found; the three pole-zero couples, three fractal derivatives α_i and the E_0. Thus, comparing the normalized errors in Tables 2 and 3 and the relative curves, it is evident that the FDGM is able to fit the real viscoelastic behavior with the minimum number of parameters for the three compounds.

It is noteworthy that the number of parameters to be identified highly affects the computational load in terms of efficiency and effectiveness. In the reported study, the same function has been used for constrained minimization problems; thus, the nature of the adopted constitutive models in terms of complexity and mathematical formulation are responsible for the variation in efficacy (ability of providing good matching with experimental data) with reasonable computing time and robustness. In light of this, the comparison between the FDGM models with the GM models points out that the FDGM is preferable because of the limited number of parameters to be determined, which means a significant reduction in frequent mathematical difficulties encountered in the ill-posed problem of identification procedures from experimental data. It should be noted that, despite the great number of parameters to be identified especially in for GM model, taking advantages form the pole-zero formulation, no convergence problems have been encountered during the identification procedure.

6. Moduli Estimation with Partial Experimental Data

In the previous section, it has been demonstrated that the FDGM is an analytical model able to fit the real viscoelastic behavior with the minimum necessary number of parameters. Furthermore, the pole-zero formulation ensures a robust and fast parameter identification process starting from the experimental data of moduli in the frequency domain. Hence, the question arises about the minimum number of experimental data needed to reproduce the materials' behavior in a wide frequency range. To carry out this study, five frequency zones have been identified in the range in which the storage modulus and the loss tangent were defined for compound A, as depicted in Figure 5. Zones 1 and 5 are, respectively, representative of the lower and upper frequencies plateau of the storage modulus. Zone 3 identifies the peak of the loss tangent curve, while zones 2 and 4 describe the curvature changing of both curves.
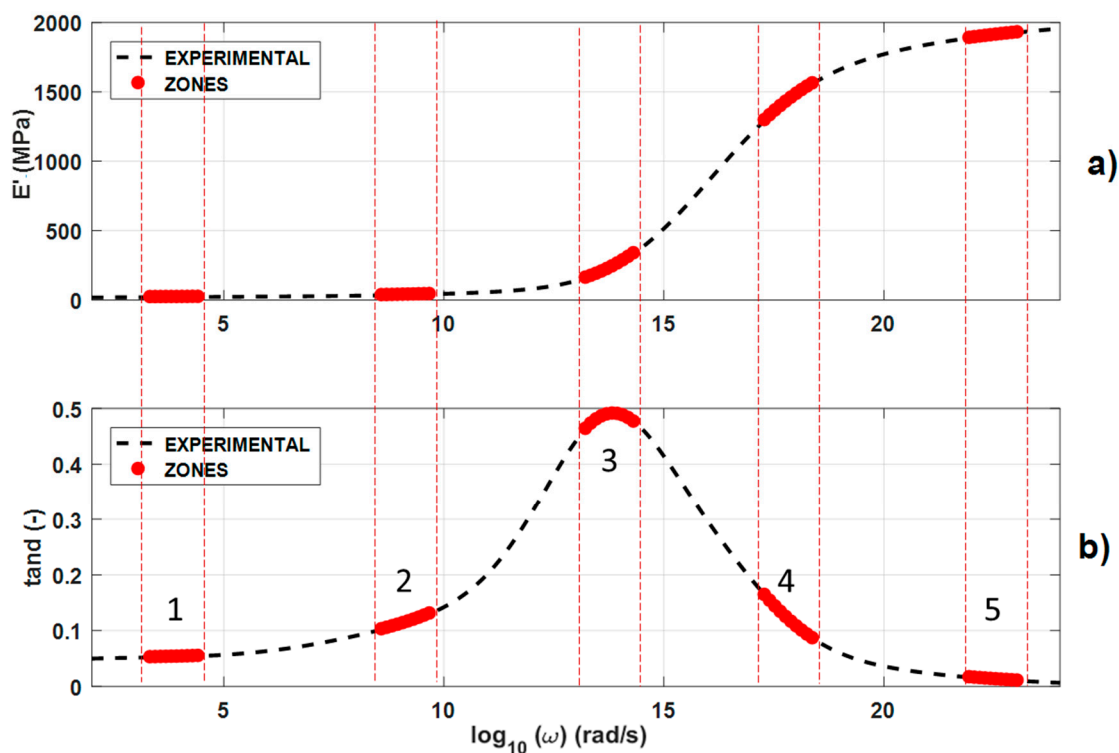

Figure 5. Definition of the five frequency zones.

The aim of the following analysis is to test the capability of the FDGM model in moduli estimation starting from a reduced set of experimental data on which to make the fitting. To pursue this aim, six different combinations of the zones defined in Figure 5 have been considered. For each combination, the parameters of the three-element FDGM have been identified and models results have been compared with the experimental ones in the entire frequency range. In Table 4, we summarize the zone combination and the relative fitting results in terms of NRMSE on the storage modulus and loss tangent while Figure 6 depicts the curves comparisons.

Table 4. NRMSE for Fractal derivative Generalized Maxwell models composed by 3, 4 and 5 elements.

Case	ZONES	NRMSE E′ (MPa)	NRMSE tanδ (-)
Combination A	1,2,3,4,5	0.004	0.035
Combination B	1,5	0.595	2.395
Combination C	1,3,5	0.004	0.066
Combination D	1,2,5	0.085	0.1695
Combination E	1,4,5	0.007	0.1640
Combination F	2,3,4	0.052	0.127

Adopting all the five zones to identify the parameters of the three-element FDGN model, it is possible to obtain an equally good fitting of the case in which all experimental data are take into account. This condition points out that the five zones chosen represent remarkable points of the curves that unequivocally determine the characteristics of a compound. Combination B results are totally insufficient to describe compound behavior, while combinations D and E fail principally in the fitting of the loss tangent. The latter result was predictable considering that, in these combinations, we did not take into account the information on the peak of the loss tangent. Combination F gives good results in the transition area of the curves, failing in both plateaus at lower and upper frequencies. Satisfying results can be achieved by combination C that, using only the data of the upper and low frequency plateaus plus the ones at the loss tangent peak, is able to fit the global compound behavior.
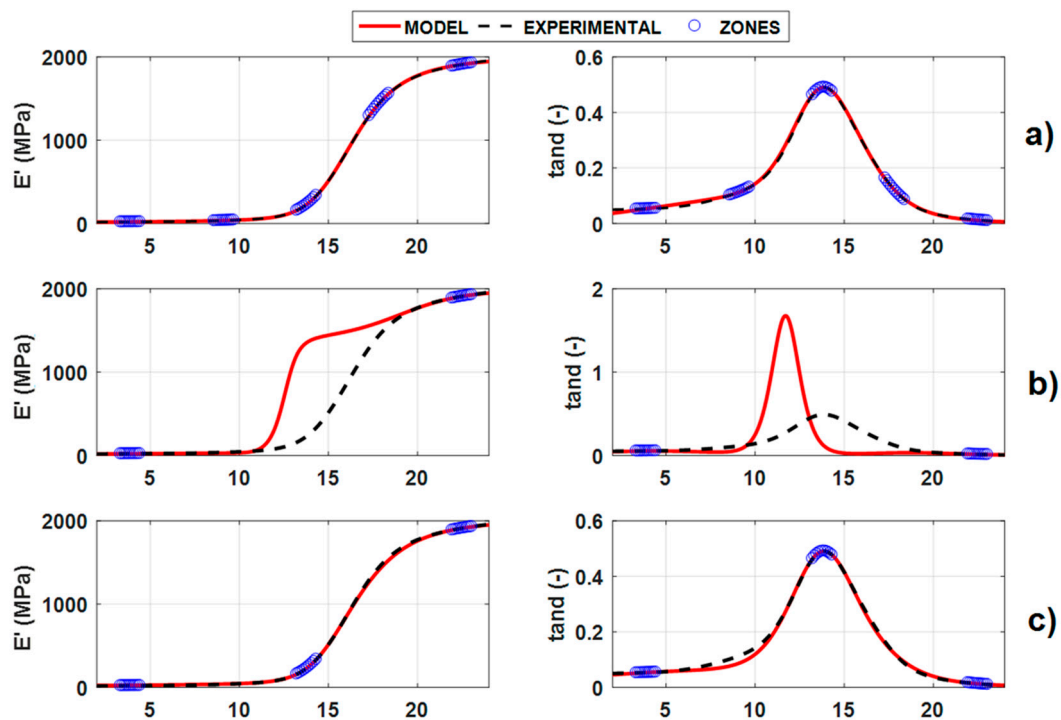
Figure 6. *Cont.*
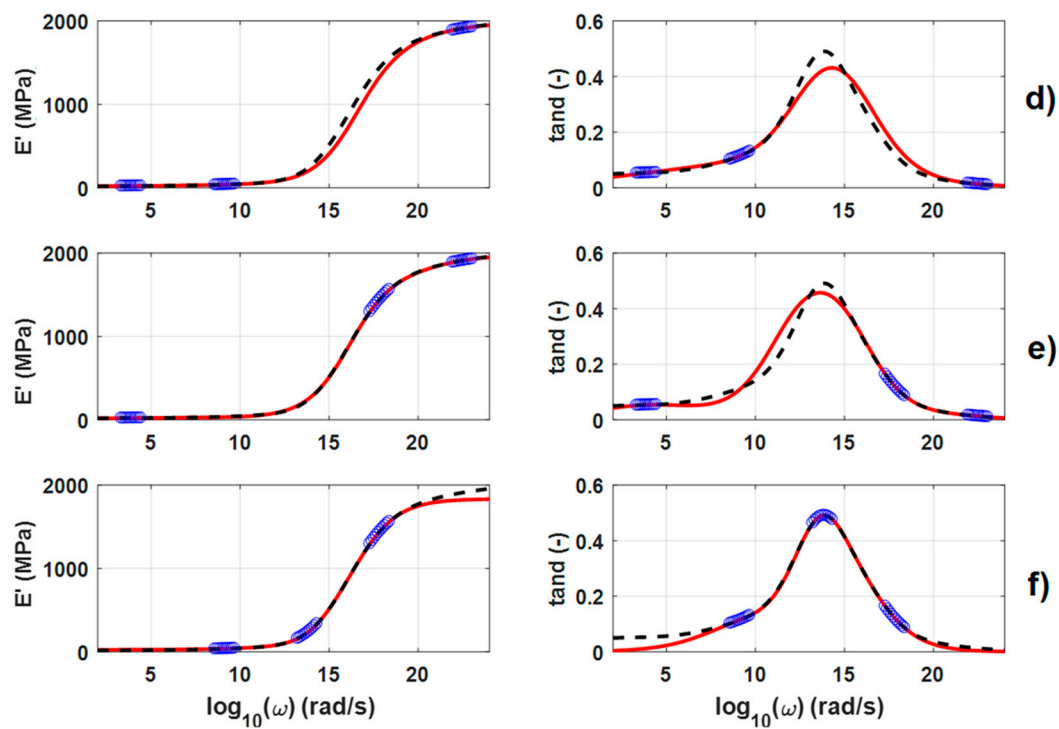
Figure 6. FDGM estimation of storage modulus and loss tangent for compound A adopting limited zones of experimental data.

7. Conclusions

The GM model and FDGM can be expressed adopting a pole–zero formulation. This formulation, that in logarithmic scale becomes a superposition of pole–zero couple behavior, allows to overcome the computational and convergence issues that occur in parameter identification of a rheological model in the time domain and frequency domain form. Thus, a constrained pole-zero identification procedure has been defined. The convenience of the pole-zero formulation in the identification of parameters of transfer functions lies in the determination of boundary conditions and initial condition of the optimization problem. Using this approach, an extensive study has been carried out to evaluate the capability of the GM and FDGM models in properly describing the viscoelastic behavior of three materials, the mechanical behavior of which was previously characterized by means of DMA tests. The analysis returns that both GM an FDGM models are able to fit the viscoelastic behavior of the compounds in the entire frequency range in which they are experimentally characterized, but the GM model needs a number of elements that are higher than the FDGM one. From a practical point of view, this means that FDGM is able to provide good matching with the simple configuration with only ten variables (three elements), while comparable results can be obtained with the GM model identifying more than 51 parameters (25 elements). Thus, comparing the normalized errors and the relative curves of the three compounds, it is observed that the FDGM is able to fit the real viscoelastic behavior with the minimum number of parameters.

The minimum number of experimental data needed to estimate the material behavior in a wide frequency range has also been investigated. The aim was to evaluate the capability of the FDGM model in moduli estimation starting from a reduced set of experimental data on which to make the fitting. An excellent prediction of the entire storage modulus and loss tangent can be obtained adopting data coming from the lower and upper frequencies plateau of the storage modulus, the peak of the loss tangent curve and the curvature changing of both curves. Furthermore, it is worth stressing that satisfying results can be achieved having also only the data available of the upper and low frequency plateaus plus the ones at the loss tangent peak.

Appendix A Parameters Values Obtained with Pole-Zero Identification Procedure

A.1. Generalized Maxwell Model Parameters

Table A1. Compound A parameters of GM models composed by 15, 25 and 35 elements.

Element	GM 15-elements		GM 25-elements		GM 35-elements	
E0 (MPa)	18.9		17.65		17.35	
	Pole	Zero	Pole	Zero	Pole	Zero
1	2.55	2.49	1.83	1.80	1.73	1.70
2	4.42	4.36	2.82	2.79	2.32	2.31
3	6.20	6.13	3.78	3.74	2.94	2.91
4	7.80	7.72	4.75	4.71	3.75	3.72
5	9.24	9.14	5.72	5.68	4.35	4.33
6	10.56	10.43	6.67	6.63	5.04	5.01
7	11.74	11.57	7.60	7.55	5.68	5.65
8	12.78	12.55	8.49	8.43	6.31	6.29
9	13.73	13.45	9.34	9.28	6.95	6.92
10	14.64	14.37	10.17	10.10	7.58	7.54
11	15.57	15.35	10.98	10.89	8.24	8.20
12	16.56	16.40	11.74	11.63	8.95	8.90
13	17.67	17.57	12.46	12.31	9.70	9.64
14	19.06	19.00	13.16	12.97	10.44	10.38
15	21.02	20.98	13.83	13.62	11.12	11.04
16			14.49	14.29	11.77	11.67
17			15.16	14.98	12.36	12.24
18			15.85	15.70	12.87	12.74
19			16.57	16.45	13.30	13.19
20			17.33	17.25	13.70	13.57
21			18.16	18.11	14.18	14.03
22			19.10	19.07	14.72	14.56
23			20.19	20.17	15.30	15.15
24			21.46	21.44	15.91	15.78
25			22.96	22.95	16.54	16.44
26					17.22	17.15
27					17.94	17.89
28					18.67	18.64
29					19.39	19.37
30					20.08	20.07
31					20.79	20.78
32					21.55	21.54
33					22.40	22.39
34					23.26	23.25
35					23.99	23.99

Table A2. Compound B parameters of GM models composed by 15, 25 and 35 elements.

Element	GM 15-elements		GM 25-elements		GM 35-elements	
E0 (MPa)	26.4		26.34		26.34	
	Pole	Zero	Pole	Zero	Pole	Zero
1	0.86	0.80	0.85	0.80	0.85	0.80
2	2.22	2.15	1.95	1.90	1.83	1.79
3	3.52	3.44	2.90	2.85	2.52	2.48
4	4.80	4.70	3.86	3.80	3.08	3.05
5	6.05	5.93	4.82	4.75	3.66	3.62
6	7.25	7.09	5.76	5.68	4.30	4.25
7	8.38	8.16	6.69	6.59	4.97	4.92
8	9.41	9.11	7.60	7.47	5.67	5.61
9	10.36	10.03	8.46	8.28	6.37	6.30
10	11.29	11.02	9.24	9.02	7.06	6.97
11	12.29	12.10	9.98	9.73	7.77	7.65
12	13.44	13.32	10.71	10.46	8.47	8.32
13	14.83	14.75	11.44	11.24	9.09	8.92
14	16.57	16.52	12.20	12.05	9.68	9.48
15	19.09	19.05	13.02	12.91	10.26	10.06
16			13.89	13.82	10.84	10.65
17			14.82	14.78	11.43	11.27
18			15.79	15.76	12.00	11.89
19			16.87	16.84	12.59	12.50
20			18.01	17.99	13.27	13.20
21			19.28	19.27	14.00	13.94
22			20.58	20.58	14.72	14.69
23			21.60	21.60	15.38	15.35
24			22.78	22.77	16.06	16.03
25			23.91	23.90	16.92	16.90
26					17.57	17.56
27					18.10	18.09
28					19.07	19.06
29					19.62	19.62
30					20.30	20.29
31					21.12	21.11
32					21.71	21.71
33					22.49	22.49
34					23.20	23.20
35					23.91	23.90

Table A3. Compound C parameters of GM models composed by 15, 25 and 35 elements.

Element	GM 15-elements		GM 25-elements		GM 35-elements	
E0 (MPa)	14.73		14.73		14.73	
	Pole	Zero	Pole	Zero	Pole	Zero
1	0.86	0.79	0.86	0.79	0.86	0.79
2	2.27	2.21	2.13	2.08	2.07	2.02
3	3.56	3.48	3.17	3.11	2.12	2.12
4	4.76	4.66	4.17	4.09	2.91	2.86
5	5.90	5.76	5.16	5.06	3.66	3.61
6	6.97	6.78	6.12	5.99	4.38	4.33
7	7.96	7.67	7.03	6.86	4.96	4.90
8	8.88	8.50	7.90	7.65	5.66	5.57
9	9.72	9.36	8.71	8.39	6.37	6.27
10	10.59	10.32	9.43	9.12	7.08	6.93
11	11.54	11.38	10.11	9.86	7.85	7.62
12	12.62	12.53	10.80	10.63	8.55	8.29
13	13.96	13.91	11.54	11.43	9.10	8.86
14	15.78	15.74	12.34	12.26	9.66	9.41
15	18.65	18.63	13.23	13.18	10.25	10.05
16			14.23	14.20	10.89	10.73
17			15.33	15.31	11.56	11.46
18			16.50	16.49	12.23	12.17
19			17.81	17.80	12.91	12.87
20			18.88	18.87	13.62	13.59
21			19.79	19.79	14.30	14.28
22			20.99	20.99	14.99	14.98
23			21.78	21.78	15.68	15.67
24			22.93	22.93	16.37	16.36
25			24.00	24.00	17.06	17.06
26					17.74	17.74
27					18.44	18.44
28					19.13	19.13
29					19.82	19.82
30					20.52	20.52
31					21.21	21.21
32					21.91	21.91
33					22.60	22.60
34					23.30	23.30
35					24.01	24.01

A.2. Fractal Derivative Generalized Maxwell Model Parameters

Table A4. Compound A parameters of FDGM models composed by 3, 4 and 5 elements.

Element	FDGM 3-elements			FDGM 4-elements			FDGM 5-elements		
E0 (MPa)	14.41			15.44			14.73		
	Pole	Zero	Gamma	Pole	Zero	Gamma	Pole	Zero	Gamma
1	12.45	5.62	0.12	2.08	1.96	0.45	3.63	1.66	0.16
2	14.53	12.45	0.40	12.60	7.37	0.14	10.55	9.06	0.24
3	16.06	14.53	0.34	14.51	12.60	0.41	15.09	12.44	0.42
4				16.16	14.51	0.32	16.67	16.05	0.40
5							19.00	18.34	0.18

Table A5. Compound B parameters of FDGM models composed by 3, 4 and 5 elements.

Element	FDGM 3-elements			FDGM 4-elements			FDGM 5-elements		
E0 (MPa)	24.82			22.41			25.19		
	Pole	Zero	Gamma	Pole	Zero	Gamma	Pole	Zero	Gamma
1	8.85	3.21	0.15	8.90	3.51	0.15	3.66	1.30	0.12
2	11.20	8.85	0.44	11.03	8.90	0.44	8.96	5.44	0.17
3	12.97	11.20	0.21	12.61	11.03	0.25	10.99	8.96	0.45
4				21.16	12.61	0.02	12.61	10.99	0.25
5							20.76	12.61	0.03

Table A6. Compound C parameters of FDGM models composed by 3, 4 and 5 elements.

Element	FDGM 3-elements			FDGM 4-elements			FDGM 5-elements		
E0 (MPa)	14.73			14.73			14.73		
	Pole	Zero	Gamma	Pole	Zero	Gamma	Pole	Zero	Gamma
1	7.46	2.26	0.12	7.62	2.23	0.12	3.66	1.30	0.12
2	10.70	7.46	0.47	10.09	7.62	0.49	8.96	5.44	0.17
3	24.45	10.70	0.02	11.13	10.09	0.32	10.99	8.96	0.45
4				24.45	11.13	0.02	12.61	10.99	0.25
5							20.76	12.61	0.03

References

1. Newell, N.; Little, J.; Christou, A.; Adams, M.; Adam, C.; Masouros, S. Biomechanics of the human intervertebral disc: A review of testing techniques and results. *J. Mech. Behav. Biomed. Mater.* **2017**, *69*, 420–434. [CrossRef] [PubMed]

2. Zhang, W.; Chen, H.Y.; Kassab, G.S. A rate-insensitive linear viscoelastic model for soft tissues. *Biomaterials* **2007**, *28*, 3579–3586. [CrossRef]

3. Peña, E.; Calvo, B.; Martínez, M.A.; Martins, P.; Mascarenhas, T.; Jorge, R.M.N.; Ferreira, A.; Doblaré, M. Experimental study and constitutive modeling of the viscoelastic mechanical properties of the human prolapsed vaginal tissue. *Biomech. Model. Mechanobiol.* **2010**, *9*, 35–44. [CrossRef] [PubMed]

4. Samali, B.; Kwok, K.C.S. Use of viscoelastic dampers in reducing wind- and earthquake-induced motion of building structures. *Eng. Struct.* **1995**, *17*, 639–654. [CrossRef]

5. Singh, M.P.; Moreschi, L.M. Optimal placement of dampers for passive response control. *Earthq. Eng. Struct. Dyn.* **2002**, *31*, 955–976. [CrossRef]

6. Park, S.W. Analytical modeling of viscoelastic dampers for structural and vibration control. *Int. J. Solids Struct.* **2001**, *38*, 8065–8092. [CrossRef]

7. Persson, B.N.J. Theory of rubber friction and contact mechanics. *J. Chem. Phys.* **2001**, *115*, 3840–3861. [CrossRef]

8. Genovese, A.; Farroni, F.; Papangelo, A.; Ciavarella, M. A Discussion on Present Theories of Rubber Friction, with Particular Reference to Different Possible Choices of Arbitrary Roughness Cutoff Parameters. *Lubricants* **2019**, *7*, 85. [CrossRef]

9. Mark, J.E. *Physical Properties of Polymers Handbook*; Mark, J.E., Ed.; Springer: New York, NY, USA, 2007.

10. Lakes, R.S. *Viscoelastic Materials*; Cambridge University Press: Cambridge, UK, 2009.

11. Liao, Z.; Hossain, M.; Yao, X.; Mehnert, M.; Steinmann, P. On thermo-viscoelastic experimental characterization and numerical modelling of VHB polymer. *Int. J. Non-Linear Mech.* **2020**, *118*, 103263. [CrossRef]

12. Dal, H.; Kaliske, M. Bergström-Boyce model for nonlinear finite rubber viscoelasticity: Theoretical aspects and algorithmic treatment for the FE method. *Comput. Mech.* **2009**, *44*, 809–823. [CrossRef]

13. Hossain, M.; Vu, D.K.; Steinmann, P. Experimental study and numerical modelling of VHB 4910 polymer. *Comput. Mater. Sci.* **2012**, *59*, 65–74. [CrossRef]

14. Amin, A.F.M.S.; Lion, A.; Sekita, S.; Okui, Y. Nonlinear dependence of viscosity in modeling the rate-dependent response of natural and high damping rubbers in compression and shear: Experimental identification and numerical verification. *Int. J. Plast.* **2006**, *22*, 1610–1657. [CrossRef]

15. Palmeri, A.; Ricciardelli, F.; De Luca, A.; Muscolino, G. State Space Formulation for Linear Viscoelastic Dynamic Systems with Memory. *J. Eng. Mech.* **2003**, *129*, 715–724. [CrossRef]

16. Bagley, R.L.; Torvik, J. Fractional calculus—A different approach to the analysis of viscoelastically damped structures. *AIAA J.* **1983**, *21*, 741–748. [CrossRef]

17. Pritz, T. Five-parameter fractional derivative model for polymeric damping materials. *J. Sound Vib.* **2003**, *265*, 935–952. [CrossRef]

18. Liu, J.G.; Xu, M.Y. Higher-order fractional constitutive equations of viscoelastic materials involving three different parameters and their relaxation and creep functions. *Mech. Time Dependent Mater.* **2007**, *10*, 263–279. [CrossRef]

19. Sasso, M.; Palmieri, G.; Amodio, D. Application of fractional derivative models in linear viscoelastic problems. *Mech. Time Dependent Mater.* **2011**, *15*, 367–387. [CrossRef]

20. Meral, F.C.; Royston, T.J.; Magin, R. Fractional calculus in viscoelasticity: An experimental study. *Commun. Nonlinear Sci. Numer. Simul.* **2010**, *15*, 939–945. [CrossRef]

21. Di Paola, M.; Pirrotta, A.; Valenza, A. Visco-elastic behavior through fractional calculus: An easier method for best fitting experimental results. *Mech. Mater.* **2011**, *43*, 799–806. [CrossRef]

22. Lewandowski, R.; Chorążyczewski, B. Identification of the parameters of the Kelvin–Voigt and the Maxwell fractional models, used to modeling of viscoelastic dampers. *Comput. Struct.* **2010**, *88*, 1–17. [CrossRef]

23. Fukunaga, M.; Shimizu, N. Comparison of fractional derivative models for finite deformation with experiments of impulse response. *J. Vib. Control* **2014**, *20*, 1033–1041. [CrossRef]

24. Khemane, F.; Malti, R.; Raïssi, T.; Moreau, X. Robust estimation of fractional models in the frequency domain using set membership methods. *Signal Process.* **2012**, *92*, 1591–1601. [CrossRef]

25. De Espíndola, J.J.; da Silva Neto, J.M.; Lopes, E.M.O. A generalised fractional derivative approach to viscoelastic material properties measurement. *Appl. Math. Comput.* **2005**, *164*, 493–506. [CrossRef]

26. Arikoglu, A. A new fractional derivative model for linearly viscoelastic materials and parameter identification via genetic algorithms. *Rheol. Acta* **2014**, *53*, 219–233. [CrossRef]

27. Shabani, M.; Jahani, K.; Di Paola, M.; Sadeghi, M.H. Frequency domain identification of the fractional Kelvin-Voigt's parameters for viscoelastic materials. *Mech. Mater.* **2019**, *137*, 103099. [CrossRef]

28. Zhou, S.; Cao, J.; Chen, Y. Genetic Algorithm-Based Identification of Fractional-Order Systems. *Entropy* **2013**, *15*, 1624–1642. [CrossRef]

29. Yuan, L.; Agrawal, O.P. A Numerical Scheme for Dynamic Systems Containing Fractional Derivatives. *J. Vib. Acoust.* **2002**, *124*, 321–324. [CrossRef]

30. Xiao, Z.; Haitian, Y.; Yiqian, H. Identification of constitutive parameters for fractional viscoelasticity. *Commun. Nonlinear Sci. Numer. Simul.* **2014**, *19*, 311–322. [CrossRef]

31. Dabiri, A.; Nazari, M.; Butcher, E.A. The Spectral Parameter Estimation Method for Parameter Identification of Linear Fractional Order Systems. In Proceedings of the 2016 American Control Conference (ACC), Boston, MA, USA, 6–8 July 2016; pp. 2772–2777.

32. Renaud, F.; Dion, J.-L.; Chevallier, G.; Tawfiq, I.; Lemaire, R. A new identification method of viscoelastic behavior: Application to the generalized Maxwell model. *Mech. Syst. Signal Process.* **2011**, *25*, 991–1010. [CrossRef]

33. Menard, K.P.; Menard, N. Dynamic Mechanical Analysis. In *Encyclopedia of Analytical Chemistry*; John Wiley & Sons, Ltd.: Chichester, UK, 2017; pp. 1–25.

34. Williams, M.L.; Landel, R.F.; Ferry, J.D. The Temperature Dependence of Relaxation Mechanisms in Amorphous Polymers and Other Glass-forming Liquids. *J. Am. Chem. Soc.* **1955**, *77*, 3701–3707. [CrossRef]

35. Koeller, R.C. Applications of fractional calculus to the theory of viscoelasticity. *J. Appl. Mech. Trans. ASME* **1984**, *51*, 299–307. [CrossRef]

36. Pintelon, R.; Schoukens, J. *System Identification: A Frequency Domain Approach, Second Edition*; Wiley: Hoboken, NJ, USA, 2012.

37.   Collantes, J.M.; Mori, L.; Anakabe, A.; Otegi, N.; Lizarraga, I.; Ayllon, N.; Ramirez, F.; Armengaud, V.; Soubercaze-Pun, G. Pole-Zero Identification: Unveiling the Critical Dynamics of Microwave Circuits beyond Stability Analysis. *IEEE Microw. Mag.* **2019**, *20*, 36–54. [CrossRef]

38.   Bland, D.R. *The Theory of Linear Viscoelasticity*; Pergamon Press: London, UK, 2019.